EuroIntervention

The impact of an eccentric intravascular ImageWire during coronary optical coherence tomography imaging

Nobuaki Suzuki[1], MD; Giulio Guagliumi[2], MD; Hiram G. Bezerra[1], MD, PhD; Vasile Sirbu[2], MD; Noah Rosenthal[1], MD; Giuseppe Musumeci[2], MD; Alessandro Aprile[2], MD; Hui Wang[3], PhD; Hiroyuki Kyono[1], MD; Satoko Tahara[1], MD, PhD; Daniel I. Simon[1], MD; Andrew Rollins[3], PhD; Marco A. Costa[1]*, MD, PhD

1. Harrington-McLaughlin Heart and Vascular Institute and Cardialysis-Cleveland Core Laboratories, University Hospitals Case Medical Center, Cleveland OH, USA; 2. Azienda Ospedaliera Ospedali Riuniti di Bergamo, Bergamo, Italy; 3. Biomedical Engineering, Case Western Reserve University, Cleveland, OH, USA

Dr. Guagliumi reports receiving grant/research support from Boston Scientific Corporation (BSC), Medtronic Vascular, LightLab Imaging and Labcoat, and is a consultant for BSC, Cordis and Volcano Corporation. Dr. Costa is on the Speaker Bureau and is a consultant for BSC, Sanofi/Aventis and Eli Lilly, and is on the Speaker Bureau and a member of the Scientific Advisory Board for Abbott, Cordis, LightLab Imaging and Scitec. Dr. Sirbu reports receiving grant/research support from LightLab Imaging. Dr. Bezerra reports receiving honoraria from LightLab Imaging. Dr Simon received research grants from Medtronic Vascular and Cordis/Johnson & Johnson. The other authors have no conflicts of interest to declare.

KEYWORDS

Coronary artery disease, optical coherence tomography, stent

Abstract

Aims: Optical coherence tomography (OCT) provides high-resolution imaging which enables characterisation of atherosclerosis and vascular response to injury, but to ensure optimal analysis, one must realise potential sources of image distortion. We designed a series of analyses, using coronary stents as a model, to investigate the influence of wire position on OCT-derived vascular images.

Methods and results: The study evaluated intracoronary OCT images from the Cardialysis-Cleveland University Hospitals Cardiovascular Imaging Core Laboratories database. Intracoronary OCT images were acquired with the M2 system (LightLab Imaging Inc., Westford, MA, USA) and analysed using a customised software. Wire concentric index (WCI) was calculated as "wire-lumen distance/lumen radius". Lumen, stent, and strut contours were defined and 360 chords (1 degree increments) were placed radially between the lumen and stent contours. Strut length was defined by the number of chords spanned by each strut. Strut level thickness (SLT) was measured with each chord. SLT variability ([Max - Min SLT]/number of chords per strut) was calculated. Lumen measurements were performed with optimal calibration and repeated with ±1% changes from optimal Z-offset. The hemisphere containing an eccentric wire had shorter strut reflections (5.0±1.6° vs. 6.6±2.1°, p<0.001) compared to the opposite hemisphere. Eccentric wires depicted 84% of the struts as non-parallel to the luminal surface (>10% SLT variability). Changing Z-offset by 1% resulted in a non-uniform shrinkage or expansion of the luminal contour in images generated from eccentric wires, but not from concentric wires.

Conclusions: Eccentric intraluminal position of the OCT ImageWire occurs frequently and affects calibration and interpretation of images, including length, orientation and visibility of vessel wall structures.

** Corresponding author: 11100 Euclid Avenue - Lakeside 3001, Cleveland, OH 44106-5038, USA*
E-mail: marco.costa@uhhospitals.org

Introduction

Imaging the endovascular environment at a micron-scale level holds considerable promise[1], but the future impact of optical coherence tomography (OCT) on clinical and research applications depends on judicious evaluation and understanding of both its strengths and intricacies. The ability of OCT to characterise arterial wall components has been demonstrated in experimental models[2]. OCT has also been used safely in humans to characterise atherosclerosis and to evaluate intravascular devices[3-6]. A recent forum among European investigators recommended the use of OCT for evaluation of drug-eluting stents (DES)[7]. However, potential sources of distortion in OCT coronary imaging reconstruction have not been previously appreciated.

The current commercially available OCT system (M2CV OCT Imaging System; LightLab Inc., Westford, MA, USA) consists of a single-mode optical fibre in a hollow rotating cable that emits light beams radially from the catheter axis. The image is reconstructed based on reflected signals of each individual scan, a process influenced by the distance between the sample and the light source. The small diameter of the ImageWire (0.019 inches) may lead to an eccentric intraluminal position during image acquisition *in vivo*, which in turn may affect image reconstruction. The present investigation aims at evaluating the influence of the ImageWire position on OCT coronary images in humans.

Methods

The study evaluated intracoronary OCT images from the University Hospitals' Cardiovascular Imaging Core Laboratories database. These images were acquired as part of clinical trials evaluating follow-up stents. The study included stents implanted electively in consecutive patients with *de novo*, long stenoses in native coronary arteries requiring overlapping stents. For the strut reflection length and orientation study, 6-month follow-up images of five lesions (zotarolimus-eluting stent: three; paclitaxel-eluting stent: one; sirolimus-eluting stent: one) were evaluated. For the strut visibility study, 6-month follow-up images of 10 lesions (zotarolimus-eluting stent: four; paclitaxel-eluting stent: four; sirolimus-eluting stent: one; bare metal stent: one) and 13-month follow-up images of 15 lesions (paclitaxel-eluting stent: 12; bare metal stent: three). The type of the stent was blinded to the analysts. Informed consent was obtained for all patients as part of their participation in the clinical trials. Stented coronary segments were selected for evaluation. This provided a good *in vivo* model to evaluate image distortion, given the stent struts' well-defined bright reflection with shadowing and known morphology. The overall goal of the study was to determine if eccentric intraluminal position of the OCT ImageWire (IW) affects calibration and image reconstruction.

OCT image analysis

Cross-sectional images (frames) were excluded from analysis if they involved a major side branch (occupying > 45 degrees), sew-up or scattered beam artifacts, or any other situation compromising image quality (Figure 1)[10]. Measurements of OCT cross-sectional images were performed using a dedicated automated contour-detection system (OCT system software B.0.1; LightLab Inc., Westford, MA, USA) developed in collaboration with the Cardialysis-Cleveland core laboratory. The lumen contour was delineated automatically, the inner and outer contours of each strut reflection were delineated semi-automatically, and an algorithm automatically placed 360 chords (1-degree increments) radially between lumen, inner and outer strut contours, and from this the distance of each chord was measured (Figure 2). These measurements form the basis of a series of assessments, each with a specific methodology, designed to address the study questions. Definitions of OCT parameters utilised in this study are described below.

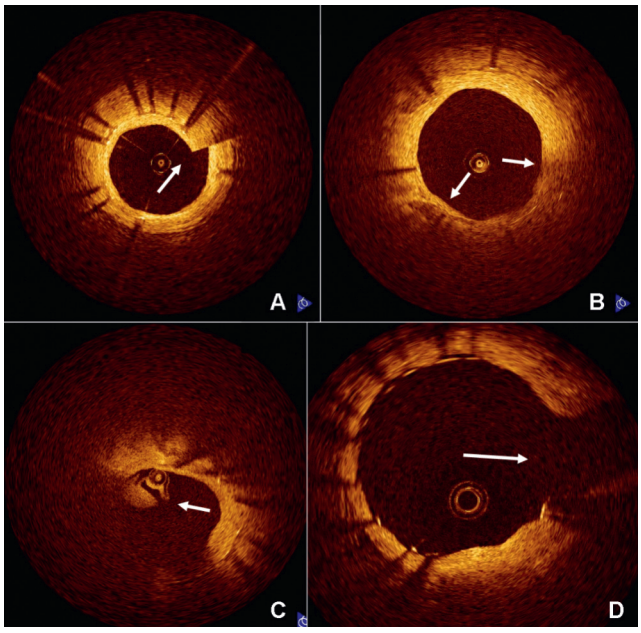

Figure 1. Examples of non-analysable frames due to common artifacts. A) Sew-up artefact (arrow) caused by the rapid axial movement of the wire during the scanning rotation, leading to the misalignment of the lumen contour. B) Scattered beam artefact caused by a bubble in the silicon lubricant between the rotating optic fibre and catheter sheath results in low signal regions which degrade penetration and resolution. C) Residual blood / thrombus, causing extensive image scattering and attenuation which impairs visualisation of the lumen contour. D) Frames were excluded when a side branch (arrow) spanned over an eighth of the total circumference.

OCT quantitative endpoints

A wire concentric index (WCI) was created as a scale of wire proximity to the lumen centre (centricity) and was calculated as the distance from the IW to the vessel wall divided by lumen radius: (WCI)=wire-lumen distance / lumen radius. In addition, the cross-sectional image was divided evenly into halves, and labelled as the hemisphere "containing" the wire or "opposite" to the wire with struts then labelled according to their location (Figures 3A & B).

Strut reflection length was measured by the number of chords (angular distance) spanning each strut reflection (Figures 3C & D). This measurement is not the true strut size, but a reflection of light (blooming) from the strut surface. Strut reflections are typically present in every quadrant of the vessel cross-sectional image, have a characteristic appearance and provide a measurable surrogate to determine how the appearance of vessel wall structures vary depending on their location in relation to the wire position.

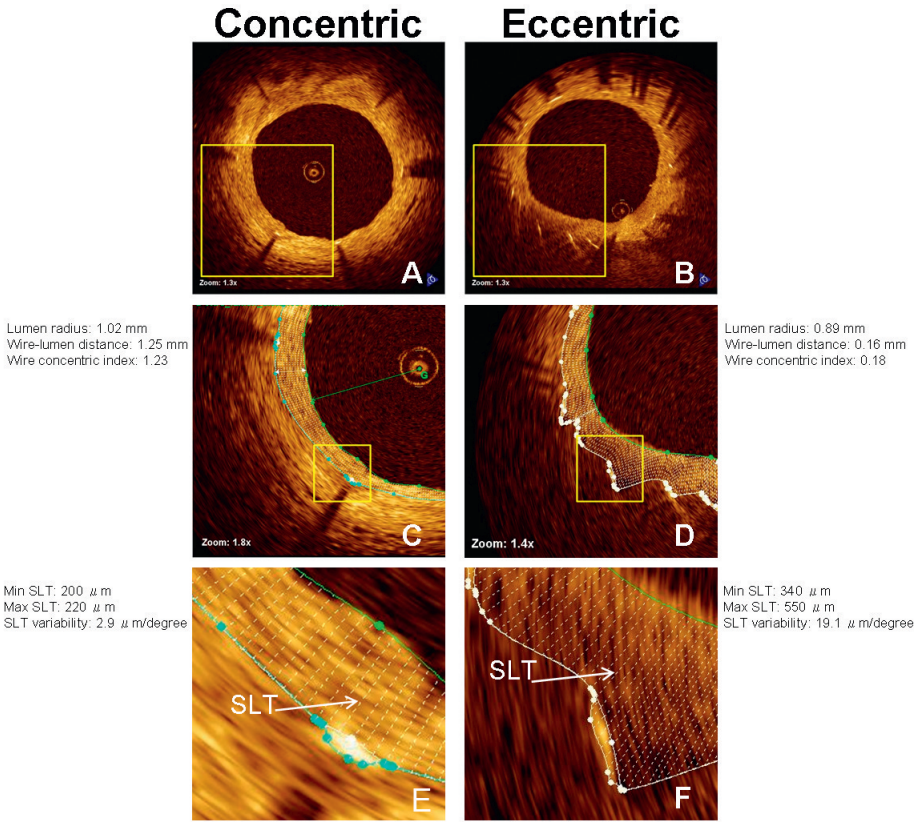

Figure 2. Evaluation of strut-level thickness variability. Representative frames with concentric (left panel) and eccentric (right panel) wire positions are shown (A, B = frames without contours). Lumen and stent contours and 360 degrees chords are shown in figures C, D, E, F. The direction of strut surface reflection is almost parallel with the lumen contour in the frame with concentric wire position (A, C, E), whereas it appears perpendicular in the frame with eccentric wire (B, D, F). The SLT variability, calculated based on each chord value spanning a single stent strut (arrows), is expected to be higher for the strut depicted in eccentric wire position (E) compared to the eccentric wire (F). SLT: strut level thickness.

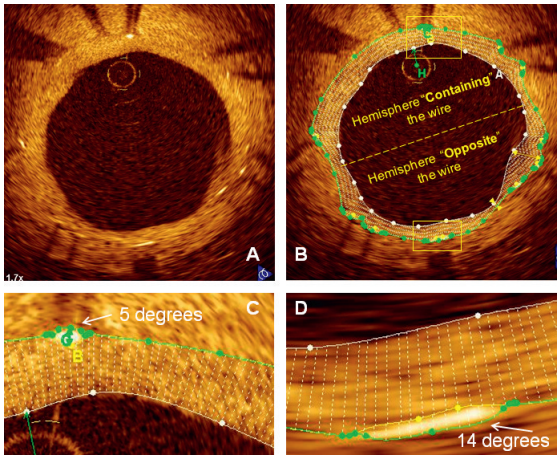

Figure 3. Evaluation of the length of strut reflection. Cross sectional OCT image with an eccentric wire without contours (A). The cross-section is divided into two hemispheres (B, contours are also depicted) based on the wire position. The strut reflection in the hemisphere opposite from the wire appears longer compared that located near the wire, which is confirmed by measurements (C and D: C shows the strut close to the wire and D shows the strut in the opposite hemisphere).

Strut-level thickness (SLT) is the distance between the inner strut contour and the coronary arterial lumen, determined automatically across the entire surface of each strut reflection at 1-degree increments (360 chords) (Figures 2C & D). SLT variability was calculated for each strut as "maximum – minimum SLT normalised (divided) by strut reflection length". This endpoint was developed to evaluate SLT as a function of WCI, and to determine if WCI affects strut orientation in space. For instance, struts with a parallel orientation to the lumen surface are expected to have minimal or no SLT variability. SLT variability >10 μm was selected based on maximum OCT resolution as an indirect index of unparallel orientation between the strut and lumen surfaces (Figures 2 E & F). To investigate the effect of wire position on strut visibility, frames were segregated in circumferential regions having the lumen center as the angle's vertex. Frames were divided into two regions: "direct" (30 degrees containing the wire and the opposite 150 degrees) and "oblique" (15 to 105 degrees on either side of the wire) regions (Figure 4). The number of visualised stent struts was compared between direct and oblique regions. Frames that had no visible struts in the "oblique" regions were considered blind frames (BF). The frequency of BF was determined as a function of WCI.

The Z-offset is an adjustable correction mechanism in OCT image calibration[11], and as part of our calibration methodology, OCT images of a guiding catheter were acquired to validate the optimal value. When calibrating the image, it is expected that the calibration affects the entire image uniformly, provided the wire is centrally located in the lumen. We performed measurements of reconstructed images using the optimal Z-offset, as determined by adjusting the fiduciary marks

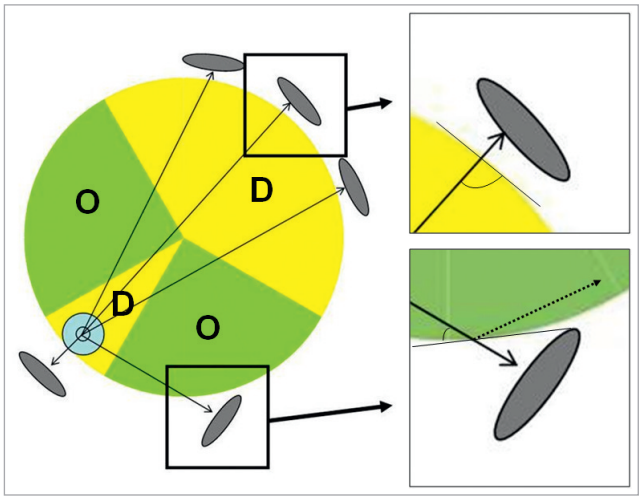

Figure 4. Graphic illustration of the vessel wall regions located in the direct and oblique orientation in relation to the IW. The stent struts are illustrated in grey oval shapes and represented according to their orientation to the lumen. The cross-section image was divided in two regions: direct ("D" = 30 degrees containing the wire and the opposite 150 degrees) vs. oblique ("O"). The right panels show the angle incidence of the beam as it enters the vessel wall in oblique and direct regions. Structure visualisation may also be affected by Snell's law[16], besides attenuation and refraction. IW: ImageWire.

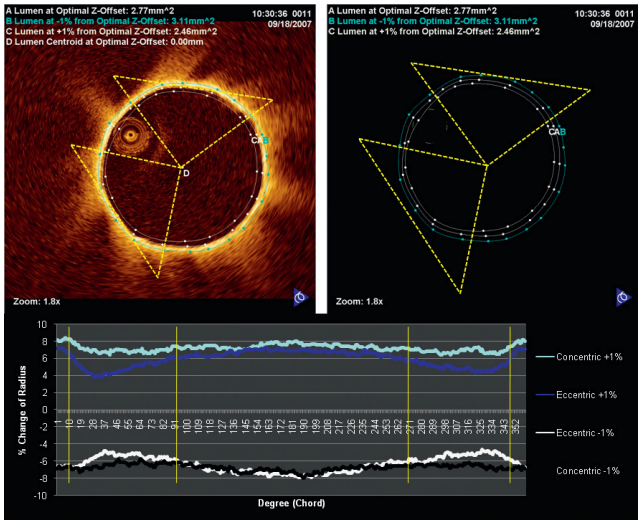

Figure 5. Impact of the wire location on image calibration. Upper panel shows a cross-sectional image without contours and the corresponding lumen contours of the same image according to the Z-offset settings (optimal-middle line, –1% outer and +1% inner contour). The regions demarcated by the yellow triangle depict the luminal contour most vulnerable to non-uniform changes in measurements with eccentric wire position. Lower panel shows a graphic display of each individual 360-degree radii measurements according to Z-offset settings and wire. The shortest distance from the centre of the catheter to the lumen wall was labelled as "0 degree" starting point. Changing the Z-offset in a concentrically placed wire (light blue and black lines) exerts a consistent change in the vessel radii. However, when the wire is eccentric (dark blue and white lines), adjusting Z-offset causes non uniform change to the radii of the vessel. Please note that the measurements start to separate (non-uniform) at approximately 10 and 270 degrees (framed by yellow lines). They correspond to the triangles in the upper panels; this region also coincides with the oblique regions depicted in Figure 4.

and then repeated measurements with +1% and –1% change in the Z-offset. We initially tested the impact of Z-offset selection on lumen areas and diameters. Then to evaluate if eccentric wire position would affect calibration of OCT images, we compared automated lumen area, diameter and 360 radii (chords) measurements in images with eccentric and concentric wire position (Figure 5).

Image acquisition

All images were obtained with an intravascular time domain OCT system (M2 Cardiology Imaging System; LightLab Imaging, Inc., Westford, MA, USA) using a 0.019-inch imaging wire (ImageWire, LightLab Imaging, Inc., Westford, MA, USA). Images were acquired during automatic-pull back at 1 mm/second and at 15.6 frames/second. The patients were given heparin intravenously before procedures to maintain an activated clotting time over 220 seconds. The OCT image system was introduced into the target coronary segment through a 6 Fr guiding catheter. A dedicated occlusion balloon catheter (Helios; Avantec Vascular Corp., Sunnyvale, CA, USA) was inflated to 0.4-0.7-atm and proximally to the target segment. During inflation the distal vessel was flushed with warm (37 ºC) heparinised Ringer's Lactate 0.5-1 cc/sec to clear the blood and assure optimal image quality. Images were digitally recorded and submitted to the corelab for offline evaluation.

Statistical analysis

For strut orientation, length, and visibility, all estimated values are shown as a continuous value, and expressed as mean standard deviation and mean with interquartile range. Comparisons of the continuous variables were made by unpaired *t*-test. Categorical values were expressed as frequencies and comparisons were made by chi-square test. Linear regression analysis was used to evaluate the correlation of WCI with Maximum SLT variability of each frame, average length of strut and strut count. Sensitivity and specificity were calculated according to standard definitions. To assess variability in delta chordal value between optimal Z-offset and ±1% Z-offset, a coefficient of variation was calculated: (the standard deviation of change in chordal length/mean change in chordal length). Differences are considered statistically significant at $p<0.05$. Statistical analyses were performed using SPSS software (Version 17; SPSS Inc. Chicago, IL, USA).

Results

Strut reflection length and orientation

Strut reflection length assessment included 420 frames with 4,025 struts. All included frames showed at least one strut reflection in the "opposite" hemisphere versus the hemisphere "containing" the wire. When the total analysed frames divided into three groups in accordance with the WCI, the wire had an eccentric location (WCI<0.22) in 147 frames, intermediate (0.22≤WCI<0.5) in 121 and concentric (WCI≥0.5) in 152 frames. Overall, strut reflection appeared longer in the "opposite" hemisphere versus the hemisphere "containing" the wire (6.6±2.1° vs. 5.0±1.6°, $p<0.001$). In frames with eccentric wire position, length of strut reflection

remained significantly different in each class of WCI (6.9±2.1° vs. 4.9±1.3° for WCI<0.22; 6.6±2.3° vs. 4.9±1.7° for WCI 0.22-0.5; 6.2±1.0° vs. 5.3±1.6° for WCI >0.5; p<0.001 for all data) in "opposite" and "containing" regions, respectively. Strut reflections remained significantly different until a WCI of ≥ 0.7 (true concentric wire position) was achieved, and thereafter the strut lengths located in the "Opposite" and "Containing" hemispheres were similar (6.1±1.7 vs. 5.7±1.9; p=0.23) (Table 1).

Strut orientation assessment included 421 frames with 4,046 struts. SLT variability >10 µm was found in 84% of frames with eccentric wires, 35.7% in intermediate, 17.3% in concentric (p<0.001). Lower WCI correlated with maximum SLT variability (r=-0.55, p<0.001).

Strut visibility

In this assessment, a total of 1,193 OCT image frames were included. There were 57 (4.8%) BFs, defined as absence of any strut. Incidence of BF for eccentric (WCI<0.29, n=431), intermediate (0.29≤WCI<0.5, n=330) and concentric (WCI≥0.5, n=432) wire positions were: 8%, 5.8%, 1.6% (p<0.001), respectively. Among frames with eccentric wire location (n=431), opposite regions depicted fewer struts than containing regions (2.6±1.6 vs. 3.6±1.8, p<0.001).

Z-offset

In this analysis, 16 catheter images were selected: eight eccentric and eight concentric wire positions. The average WCI was 0.26±0.03 and 0.56±0.18 (p<0.001) in the eccentric and concentric group respectively. Changing the Z-offset by +1% affected the average diameter of all frames by 6.5% and cross-sectional area by 13.5%. Changing the Z-offset by –1% affected the average diameter of all frames by -6.5% and cross-sectional area by –12.4%. However, the relative difference in measurement change between concentric and eccentric frames was significant (Table 2). Further, these changes in radii measurements were not uniformly distributed around the lumen (i.e., the image did not shrink or expand equally) with eccentric wire position. Depicted graphically, the average degree of change for each chord is shown; the corresponding region which is most inconsistently affected is indentified between the yellow lines (Figure 5). In the +1% Z-offset group, the coefficient of variation for radial change was 23.8 (eccentric) compared to 6.26 (concentric). For the –1% Z-offset group, the coefficient of variation was –17.1 (eccentric) compared to –5.64 (concentric). Interestingly, regions approximately between 10-90 degrees and 270-350 degrees showed the most discrepancy in change among the 360 chords of the circle. Ultimately this resulted in a deformation of the lumen / vessel contour as seen in the contour-only image (figure 5 upper-right panel).

Table 2. Wire concentricity and measurement.

		Concentric	Eccentric	*P* value
WCI		0.56	0.26	<0.001
Diameter	Optimal	1.83	1.85	0.611
	Z-Offset+1%	1.7	1.74	0.239
	Z-Offset-1%	1.95	1.96	0.794
	%change optimal to +1%	7.18	5.84	<0.001
	%change optimal to –1%	6.76	6.3	0.08
Area	Optimal	2.64	2.69	0.71
	Z-Offset+1%	2.27	2.38	0.254
	Z-Offset-1%	3.01	3.02	0.805
	%change optimal to +1%	13.8	11.5	0.001
	%change optimal to –1%	14	12.8	0.022

WCI: wire concentric index

Discussion

OCT is a novel imaging modality with an expanding role for *in vivo* evaluation of coronary arteries, and an emerging niche in the assessment of coronary artery plaque, stent apposition and device evaluation. With the increasing usage of OCT, it is important to recognise a potential source of image bias in the production of these high resolution vascular images. The effect of eccentric wire position has been an under-appreciated source of potential error, although similar effects have already been indicated in the frontier studies on intravascular ultrasound[12]. The results of this study indicated that an eccentric intraluminal position of the OCT IW affects image calibration, visibility, perceived orientation and measured length of structures located within the vessel wall (i.e., stent strut reflections). Recognition of these and other sources of distortion in image interpretation can cause the incorrect evaluation of incomplete stent apposition and are critical for both clinical and research applications of OCT.

As shown in Table 3, there are various artifacts of intracoronary OCT images other than we investigated in the current study. One should pay attention all of them for the accurate interpretation of the OCT images. Eccentric wire position leads to significant changes in strut length and orientation. Such image misrepresentation reveals that one must take into account the distance between the object and IW as well as its location in relation to the wire position. Additionally, the effect of rotational scanning on image reconstruction has two other

Table 1. Strut reflection length as a function of wire eccentricity.

WCI	Average "opposite" strut length		Average "containing" strut length		p
	Mean±SD	Median (IQR)	Mean±SD	Median (IQR)	
<0.22 (n=147)	6.9±2.1	6.5 (5.4, 7.7)	4.9±1.3	4.8 (4.0, 5.6)	p<0.001
0.22-0.5 (n=121)	6.6±2.3	6.0 (5.1, 7.3)	4.9±1.7	4.5 (4.0, 5.5)	p<0.001
>0.5 (n=152)	6.2±1.9	5.7 (5.0, 7.0)	5.3±1.6	5.0 (4.2, 5.8)	p<0.001
		Highly concentric wire placement			
<0.7 (n=358)	6.7±2.2	6.0 (5.2, 7.4)	4.9±1.4	4.7 (4.0, 5.5)	p<0.001
≥0.7 (n=62)	6.1±1.7	5.8 (5.0, 6.9)	5.7±1.9	5.3 (4.5, 6.4)	p=0.23

WCI: wire concentric index

Table 3. Artefacts of intracoronary OCT.

Increased lateral resolution (merry-go round effect)	Investigated in the article.
Odds orientation of high signal structures (sunflower artefact)	Investigated in the article.
Signal attenuation for beam reflection and refraction	Investigated in the article.
Inappropriate Z-offset	Investigated in the article.
Beam reverberation	Described in the article.
Axial movement of ImageWire (Sew-up artefact)	Described in the article.
Signal loss for residual blood	Described in the article.
Saturation artefact	Some scan line can show the streaked appearance.
Microbubble effect	Microbubbles can be contained in the silicon layer inside of ImageWire. First, microbubbles can disrupt the beam and cause the decrement of signal backwards. Second, beam distortion can be caused and a pseudo-structure may appear because of the rationale of a side lobe artefact[17].
Beam divergence	OCT signal can depend on the difference in focus point and Rayleigh range.
Non-uniform pullback owing to heart beat	Because of the longitudinal movement of image wire owing to heart beat, automated pullback speed may not be uniform, and some regions of the vessel may be skipped and out of image acquisition.

potential sources of bias that likely contributed to this intracoronary imaging phenomenon, as described below.

"Sunflower effect" – object orientation

Coronary OCT images are a reconstruction of multiple scans (A lines) obtained while the IW spins, emitting light and being pulled along the artery. All structures thus appear in the direction of the spinning wire and perpendicular to the emitted beam from the wire, not perpendicular to the centroid of the lumen. If the wire is in a concentric position, the centre of the true image and displayed images are similar, but this relationship is affected by an eccentric wire position.

A by-product of rotational scanning, the reflections from metallic stent struts can be elongated and seemingly align toward the IW, akin to sunflowers aligning to the sun. This effect is pronounced with eccentric wire position, as it can display strut reflections almost perpendicular to the lumen surface in oblique regions from the wire. Besides its distinct visual appearance, this phenomena is quantified in our study by the high SLT variability observed in the oblique regions in eccentric wires (Figures 2E & F). Such effects can also be seen in intravascular ultrasound (IVUS) images, however the lower resolution of IVUS precludes strut-level analyses, and the larger IVUS catheter is usually more centrally located within the lumen. This effect will likely be diminished with the newer generation of optical frequency domain imaging (OFDI) OCT because of a larger catheter size, however this concept still needs to be tested. When using wire-based OCT platforms, one should be aware of the potential impact of sunflower artifacts during stent and plaque analyses particularly in frames with eccentric wires. In our corelab, when performing SLT analysis, great attention is paid to placing measurements in the middle of the blooming artifacts to minimise the influence of the "sunflower effect" on the SLT results.

"Merry-go-round effect" – object length

OCT's high axial resolution is well-known, but its lateral resolution is limited by the number of scans (A lines, 200). Thus, distance dependant image distortion may also occur with rotational scanning. As such, the further the distance of the object (i.e., strut) from the IW, the longer its angular length appears. This phenomenon is secondary to the effect of lateral resolution in regions far from the "sweet-spot" focus, and away from the light source. One may correlate these images with "merry-go-round" physics, as objects farther from the central axis "move" faster than near field objects and produce a "stretched" image. We propose that this may have important future implications in the serial assessment of strut length, particularly when evaluating the degradation of bioabsorbable stents. From the result of this study, WCI of ≥ 0.7 should be optimal for the correct evaluation of strut length.

Strut visibility

The effect of beam angle and distance from the image catheter on echogenicity between adventitia and media has been reported in IVUS[13]. Similarly, beam angle and distance from the IW may affect the OCT signal. This study demonstrated that strut visibility can be suboptimal in particular regions of the cross-sectional image, a characteristic more evident when the wire position is eccentric. The greater number of stent struts imaged in the direct ("D") vs. oblique ("O") regions suggests the potential to "miss" structures in the coronary artery wall in the regions least perpendicular (oblique) to the image beam.

Light attenuation is a well known phenomenon affecting signal intensity in OCT image. Together with refraction, these are the main factors leading to relatively poor OCT image depth. In eccentric wires, the light will travel through tissue to image the oblique wall regions. Tissue has much higher attenuation and refraction indexes than the lumen filled with saline or contrast. One should be aware that low or lack of signal in plaques located in regions oblique to eccentric wires can be explained by the intrinsic properties of OCT rather than the presence of calcium or lipid components.

Z-offset

The observed changes in lumen dimensions according to the Z-offset settings highlight the importance of accurate calibration for OCT image measurements, which is similar to other imaging modalities. Importantly, our 360 chord (every 1-degree) circumferential analysis showed that the image shrinks or expands in a non-uniform manner along the lumen circumference if the wire is eccentric. Comparing an eccentrically placed wire to a concentric one, the impact of changing Z-offset is significantly different in the contour of the wall near to the IW. Regions located in an oblique orientation adjust less to changes in Z-offset, which in extreme cases creates a visual luminal distortion. Importantly, this happens in a similar location (oblique regions) to the loss of visualised stent struts and sunflower artifacts. Interpreters of OCT images should be aware of these "hot-spots", located at 15-105

degrees on either side of an eccentric IW, where distortion congregates. When the catheter is concentric, changing Z-offset affects all regions of the lumen nearly equally (uniformly). The magnitude (±1%) of the changes in Z-offset tested in this study demonstrate a proof of concept, although it is larger than would typically occur in a corelab and with well trained users in the clinical setting. However, inexperienced operators should be aware of the critical impact of Z-offset settings for accurate measurements and image visualisation when performing online analyses, as a 12-14% difference in area may impact clinical decision making, particularly in moderate stenoses. While it is not yet known if this has clinical relevance, our study highlights the importance of careful evaluation of optimal Z-offset, given the potential for contour distortion and potential misinterpretation of structures.

Limitations

The current study did not test the impact of pull-back speed and difference in the type of stent on these artifacts, although the previous paper showed these effects[14,15]. The present findings are not necessarily applicable to OFDI OCT systems, since both physics of the light source and mechanics of the catheter including different catheter profile may have significant impact on the image formation.

Conclusion

The present study shows different types of image production distortions and reveals their amplification as a result of an eccentrically placed IW. The WCI index was found to correlate with the various artifacts demonstrated (object length, orientation, luminal contour, as well as the ability to depict objects at obtuse angles to the image beam). Eccentric wire position was also shown to impart image distortion during the calibration of the system. Physicians and scientists must be aware of these fundamental concepts for the optimal use and proper interpretation of OCT images in both clinical and research applications.

References

1. Fujimoto JG, Boppart SA, Tearney GJ, Bouma BE, Pitris C, Brezinski ME. High resolution in vivo intra-arterial imaging with optical coherence tomography. *Heart.* 1999;82:128-33.

2. van der Meer FJ, Faber DJ, Perree J, Pasterkamp G, Baraznji Sassoon D, van Leeuwen TG. Quantitative optical coherence tomography of arterial wall components. *Lasers Med Sci.* 2005;20:45-51.

3. Guagliumi G, Sirbu V. Optical coherence tomography: high resolution intravascular imaging to evaluate vascular healing after coronary stenting. *Catheter Cardiovasc Interv.* 2008;72:237-47.

4. Jang IK, Tearney GJ, MacNeill B, Takano M, Moselewski F, Iftima N, Shishkov M, Houser S, Aretz HT, Halpern EF, Bouma BE. In vivo characterization of coronary atherosclerotic plaque by use of optical coherence tomography. *Circulation.* 2005;111:1551-5.

5. Bouma BE, Tearney GJ, Yabushita H, Shishkov M, Kauffman CR, DeJoseph Gauthier D, MacNeill BD, Houser SL, Aretz HT, Halpern EF, Jang IK. Evaluation of intracoronary stenting by intravascular optical coherence tomography. *Heart.* 2003;89:317-20.

6. Courtney BK, Munce NR, Anderson KJ, Thind AS, Leung G, Radau PE, Foster FS, Vitkin IA, Schwartz RS, Dick AJ, Wright GA, Strauss BH. Innovations in imaging for chronic total occlusions: a glimpse into the future of angiography's blind-spot. *Eur Heart J.* 2008;29:583-93.

7. Daemen J, Simoons ML, Wijns W, Bagust A, Bos G, Bowen JM, Braunwald E, Camenzind E, Chevalier B, Dimario C, Fajadet J, Gitt A, Guagliumi G, Hillege HL, James S, Juni P, Kastrati A, Kloth S, Kristensen SD, Krucoff M, Legrand V, Pfisterer M, Rothman M, Serruys PW, Silber S, Steg PG, Tariah I, Wallentin L, Windecker SW, Aimonetti A, Allocco D, Baczynska A, Bagust A, Berenger M, Bos G, Boam A, Bowen JM, Braunwald E, Calle JP, Camenzind E, Campo G, Carlier S, Chevalier B, Daemen J, de Schepper J, Di Bisceglie G, Dimario C, Dobbels H, Fajadet J, Farb A, Ghislain JC, Gitt A, Guagliumi G, Hellbardt S, Hillege HL, Ten Hoedt R, Isaia C, James S, de Jong P, Juni P, Kastrati A, Klasen E, Kloth S, Kristensen SD, Krucoff M, Legrand V, Lekehal M, Lenarz L, Ni Mhullain F, Nagai H, Patteet A, Paunovic D, Pfisterer M, Potgieter A, Purdy I, Raveau-Landon C, Rothman M, Serruys PW, Silber S, Simoons ML, Steg PG, Tariah I, Ternstrom S, Van Wuytswinkel J, Waliszewski M, Wallentin L, Wijns W, Windecker SW. ESC Forum on Drug Eluting Stents European Heart House, Nice, 27-28 September 2007. *Eur Heart J.* 2009;30:152-61.

8. Guagliumi G, Musumeci G, Sirbu V, Bezerra HG, Suzuki N, Fiocca L, Matiashvili A, Lortkipanidze N, Trivisonno A, Valsecchi O, Biondi-Zoccai G, Costa MA; ODESSA Trial Investigators. Optical coherence tomography assessment of in vivo vascular response after implantation of overlapping bare-metal and drug-eluting stents. *JACC Cardiovasc Interv.* 2010; 3:531-9.

9. Guagliumi G, Sirbu V, Costa M, Musumeci G, Trivisonno A, Matiashvili A, Lortkipanidze N, Mihalcsik L, Valsecchi O, Suzuki N, Coletta J, Mintz GS, Maehara A, Parise H, Lansky AJ, Cristea E, Mehran R, Stone GW. Long-term Strut Coverage of Paclitaxel Eluting Stents Compared to Bare-Metal Stents Implanted During Primary PCI in Acute Myocardial Infarction. A Prospective, Randomized, Controlled Study Performed with Optical Coherence Tomography. HORIZONS-OCT. Paper presented at: Late Breaking Trials, American Heart Association Annual Meeting; November 15, 2008; New Orleans, LA.

10. Bezerra HG, Costa MA, Guagliumi G, Rollins AM, Simon DI. Intracoronary optical coherence tomography: a comprehensive review clinical and research applications. *JACC Cardiovasc Interv.* 2009;2:1035-46.

11. Suzuki N, Coletta J, Guagliumi G, Costa MA. Clinical Applications of OCT. In: Lemos PA, ed. Diagnostic Methods In The Cardiac Catheterization Laboratory: A Practical Approach for Special Clinical Situations. London: Informa Healthcare; 2009.

12. Di Mario C, Madretsma S, Linker D, The SH, Bom N, Serruys PW, Gussenhoven EJ, Roelandt JR. The angle of incidence of the ultrasonic beam: a critical factor for the image quality in intravascular ultrasonography. *Am Heart J.* 1993;125:442-8.

13. Courtney BK, Robertson AL, Maehara A, Luna J, Kitamura K, Morino Y, Achalu R, Kirti S, Yock PG, Fitzgerald PJ. Effects of transducer position on backscattered intensity in coronary arteries. *Ultrasound Med Biol.* 2002;28:81-91.

14. Negi N, Koto M, Shite J, Sawada T, Kawamitsu H. Examination of accuracy and factors influencing optical coherence tomography (OCT) measurements. *Nippon Hoshasen Gijutsu Gakkai Zasshi.* 2009;65:1041-7.

15. Sawada T, Shite J, Negi N, Shinke T, Tanino Y, Ogasawara D, Kawamori H, Kato H, Miyoshi N, Yoshino N, Kozuki A, Koto M, Hirata K. Factors that influence measurements and accurate evaluation of stent apposition by optical coherence tomography. Assessment using a phantom model. *Circ J.* 2009;73:1841-7.

16. Beek JF, Faber DJ. An introduction to tissue optics for OCT. In: Regar E, Van Leeuwen TG, Serruys PW, eds. Optical Coherence Tomography in Cardiovascular Research. London: Informa Healthcare; 2007:3-18.

17. Suzuki N, Yamamoto H, Ishikawa S, Shiratori Y, Miyazawa A, Kozuma K, Isshiki T. Impact of the Beam Distortion on the Quantitative Coronary Artery Optical Coherence Tomography Analysis. Paper presented at: SPIE Bios; January 23, 2010; San Francisco, CA.